Materials Chemistry and Physics 252 (2020) 123422

Contents lists available at ScienceDirect

Materials Chemistry and Physics

journal homepage: www.elsevier.com/locate/matchemphys

Enhanced thermal conductivity in diamond/copper composites with tungsten coatings on diamond particles prepared by magnetron sputtering method

Jinhao Jia, Shuxin Bai *, Degan Xiong, Jing Xiao, Tingnan Yan

College of Aerospace Science and Engineering, National University of Defense Technology, Changsha, 410073, China

HIGHLIGHTS

- The magnetron sputtering is a feasible approach to prepare controllable tungsten coatings for the diamond/Cu composites.
- Effect of the tungsten coatings on properties of the diamond/Cu composites was studied.
- The diamond/Cu composites exhibited an excellent TC of 8796 ± 11 W m^{-1} K^{-1} and a fine gas tightness of 2.1 × 10^{-10} Pa m^3 s^{-1}

ARTICLE INFO

Keywords:
Diamond/Cu composites
Tungsten coating
Microstructure
Thermal conductivity

ABSTRACT

Tungsten coatings of 45–300 nm thickness were sputtered deposited on diamond particle surfaces, and diamond/Cu composites were obtained through pressureless infiltration of liquid copper into a bed of coated diamond particles. The composition of the as-deposited coatings was investigated. The effects of coating characteristics on the microstructure, gas tightness and thermal conductivities (TC) of the diamond/Cu composite were also discussed. Results showed that the originally smooth diamond surface are uniformly covered by nanosized tungsten cone arrays. Tungsten coatings with a thickness above 93 nm was found to be the most effective in improving the densification of overall composites and minimizing the interface thermal resistance between reinforcement and matrix. The thermal conductivity of composites reached 731 ± 10 W m^{-1} K^{-1} with a 300 nm tungsten coating and achieved a maximum of 796 ± 11 W m^{-1} K^{-1} with 218 nm coating. In addition, the interface thermal resistance between matrix and coated diamond particles was discussed in accordance with the calculations using a theoretical model.

1. Introduction

Diamond/Cu composites have been extensively studied as a good candidate for three-dimensional integration communication device packing materials due to its excellent thermophysical properties [1–3]. To further improve the mechanical and physical properties of diamond/Cu, it is essential to optimize the interfacial bonding. Some approaches involved alloying Cu with minor amounts of carbide of carbide formers [4–7], but non-metallic elements are unfavourable for developing the full potential of metal matrix, even resulting in noticeably reduced physical and mechanical properties of the composite. Electrodeposition has been used to fabricate diamond/Cu composites, but microstructure defects are common in a combined interface [8,9]. In addition, although high temperature and high pressure technique can minimize the interfacial thermal resistance, it cannot realise the near-net shape of diamond/Cu composite with complex structures [10]. The surface metallisation of diamond particles with carbide-forming metals, such as W, Cr, Mo, and Ti, has been effective in overcoming these obstacles [11–16]. They could preserve the intrinsic merits of the metal matrix coupled with property optimisation in diamond/Cu composites. Compared with TiC, Mo_2C and B_4C coatings, a single-layered WC coating could substantially improve the performance of diamond/Cu, and TC values over 700 W m^{-1} K^{-1} was achieved through the WC-coated diamond/Cu composites filled with a particle volume fraction of approximately 62% [17–19]. However, most cases applying coatings onto diamond are fabricated using a diffusion method or salt bath treatment. In both cases, the diamond carbon reacts with substances or is easily oxided at high temperature, and obtaining a thin and

* Corresponding author.
E-mail address: shuxinbai@foxmail.com (S. Bai).

https://doi.org/10.1016/j.matchemphys.2020.123422
Received 2 September 2019; Received in revised form 9 May 2020; Accepted 13 June 2020
Available online 18 June 2020

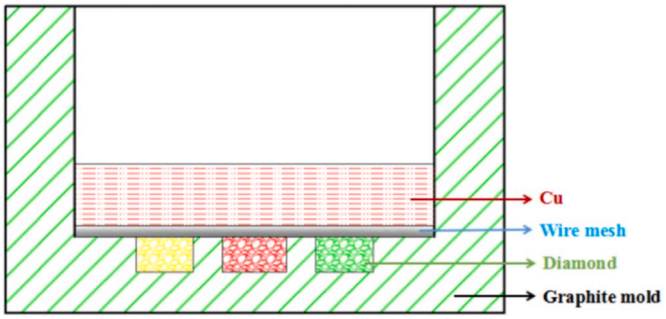

Fig. 1. Schematic representations of the assembly unit.

controllable interfacial carbide layer is unlikely due to the nonuniform nucleation on the diamond surface [20,21]. Abyzov et al. [16,18] found that the diamond/Cu composite presented thermal conductivities ranging from 552 ± 6 W m^{-1} K^{-1} to 686 ± 8 W m^{-1} K^{-1} when tungsten based coating with a thickness of 260 nm is introduced onto diamond particles via diffusion method. However, the thickness of the tungsten based coating was thicker than the expectation. They concluded that the optimal values of tungsten based coating thickness for preparing diamond-Ag (Cu) composites range from 100 nm to 250 nm. And the modified layer includes tungsten and tungsten carbide caused by the reaction between coating and diamond during the preparation process. The critical issue is controlling the coatings precisely to maintain a minimum interfacial thermal resistance. Magnetron sputtering has been proved to be useful for preparing uniform and controllable thickness coatings [19,22,23]. Chen et al. [24] prepared tungsten coating by the magnetron sputtering method and no significant debonding was observed in diamond/Al composites with 45 nm and thicker tungsten coatings. Yang et al. [14] investigated the effect of tungsten coatings on the TC value of diamond/Al composites and found that magnetron sputtering was feasible for preparing reliable tungsten coatings for diamond/Al composites. Although magnetron sputtering is an novel strategy to prepare thickness-controllable coatings, the effect of tungsten-coating prepared by the magnetron sputtering method for the diamond/Cu composites has not been systematically investigated.

In the present work, in order to further optimize the performance of diamond/Cu composites, DC magnetron sputtering was applied to deposit tungsten coatings with a thickness range of 45–300 nm on diamond

Table 1
Experimentally measured values of Gas tightness and thermal conductivity for the three diamond/Cu Composites.

Composites	Coatings thickness (nm)	Tungsten to carbon mass ratio	Thermal conductivity (W·m^{-1}·K^{-1})	Gas tightness (Pa·m^3·s^{-1})	R_C (m^2·KW^{-1})	
					H-J	ideal value
A	45	0.021	500 ± 13	5.1×10^{-8}	2.00×10^{-7}	0.77×10^{-9}
B	93	0.043	690 ± 8	8.5×10^{-9}	7.20×10^{-8}	1.03×10^{-9}
C	218	0.061	796 ± 11	7.1×10^{-10}	3.75×10^{-8}	1.66×10^{-9}
D	300	0.076	731 ± 10	2.1×10^{-10}	6.05×10^{-8}	2.24×10^{-9}

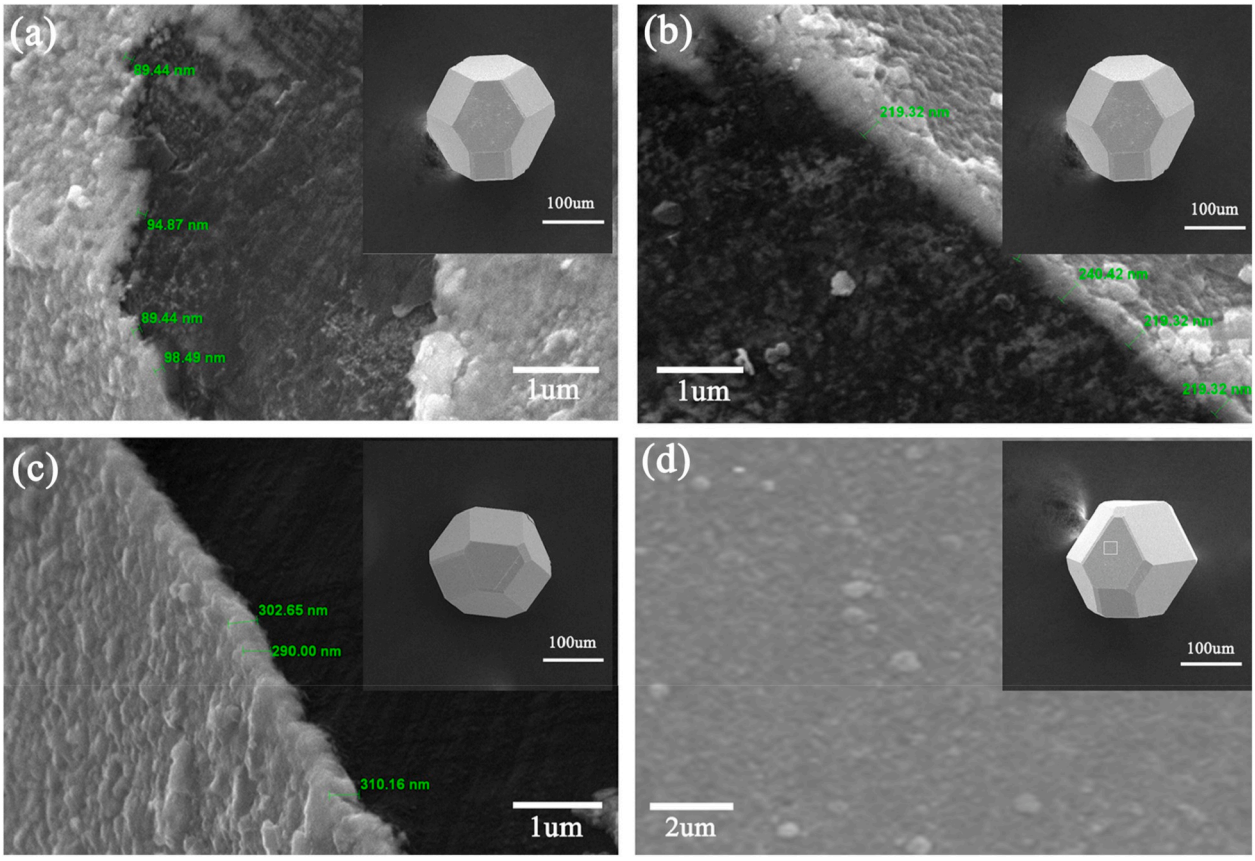

Fig. 2. Typical cross-section view image: diamond particles magnetron sputtered for (a) 180min, (b) 360min and (c) 540min, (d) SEM images of diamond particles magnetron sputtered for 90min.

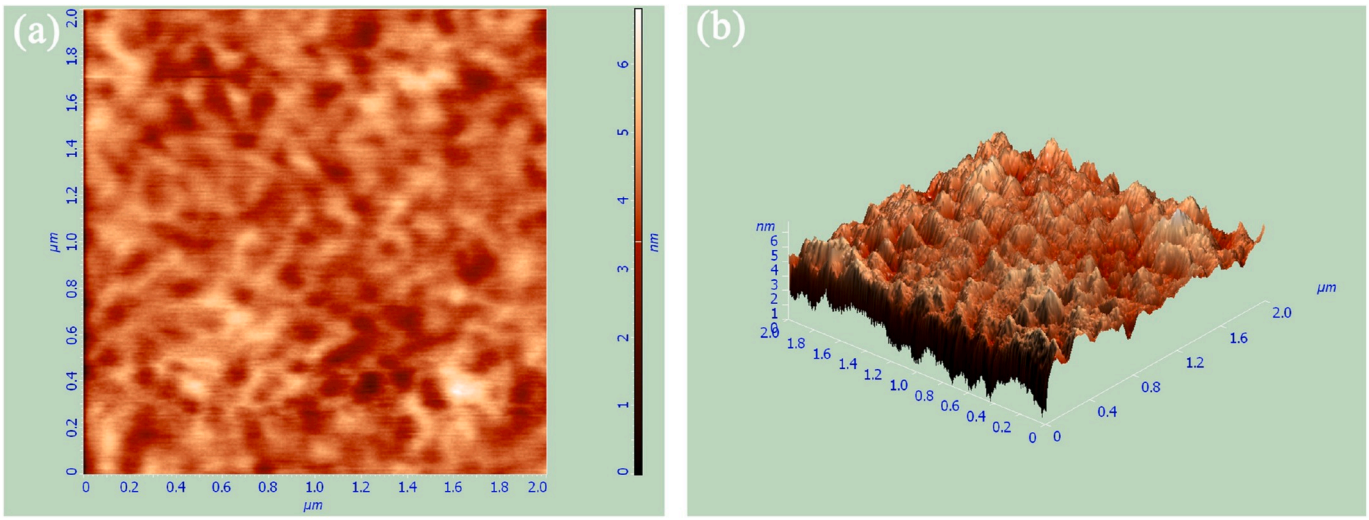

Fig. 3. AFM observation the surface of as-deposited tungsten on diamond particles surface; (a) Two-dimensional phase image, (b) three-dimensional topographical image.

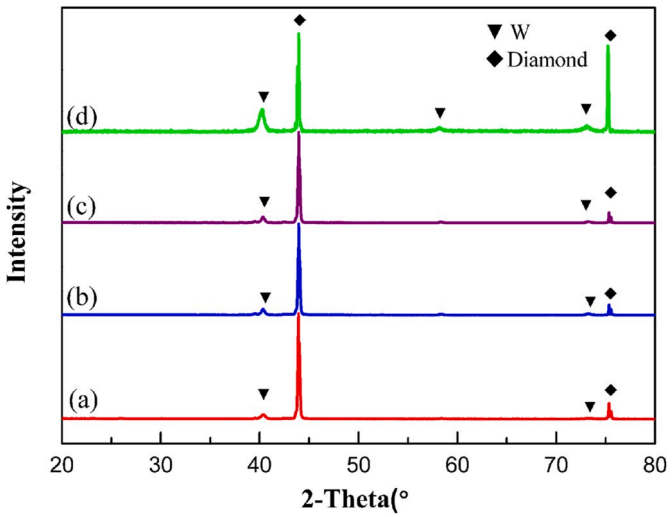

Fig. 4. XRD analysis of the diamond particles with various tungsten coatings: (a) 45 nm, (b) 93 nm, (c) 218 nm, (d) 300 nm.

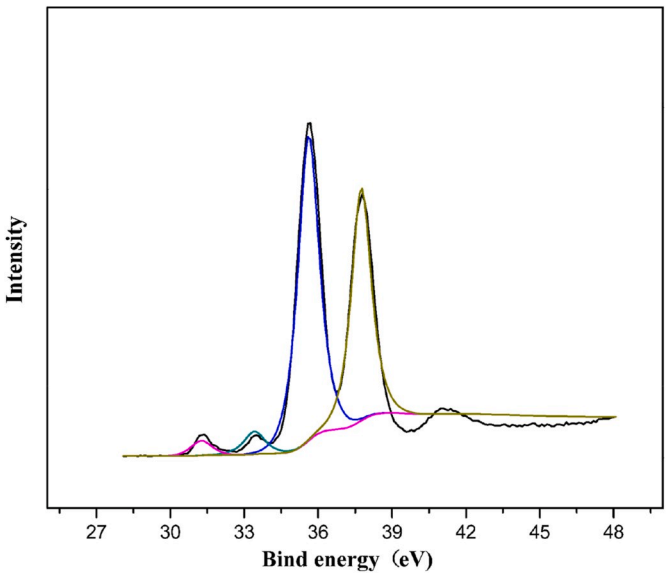

Fig. 5. XPS patterns of diamond particles coated with 45 nm tungsten.

particles. The composition and morphological characteristics of as-deposited coatings were investigated. The main objective was to fabricate Cu/diamond composites with different interfaces and analyse the effect of coatings with different characteristics on the microstructure and thermal conductivity properties of the Cu/diamond composites. Meanwhile, the interface thermal resistance was theoretically analysed to account for the thermal conductivity behavior.

2. Experimental

Synthetic hexagonal or octahedral diamond particles (HWD40) with a diameter of 150–180 μm and commercial purity oxygen-free Cu (>99.99 wt%) were used as raw materials. A tungsten metal target (99.95%) with dimensions of 100 mm × 5 mm and a grain size of 300 μm was used for the deposition of tungsten atoms in the experiments.

Tungsten atoms were deposited on diamond particles using a JGCF-600 DC magnetron sputtering system (Beijing Taikono Technology Co., Ltd., China). This system was equipped with a rotary sample holder to prepare controllable coatings on the surface of diamond particles. The temperature in the holder was 300 °C and monitored by a thermocouple. For each magnetron sputtering process, 300 g of cleaned diamond was placed into a sample holder which was rotated at 45 rpm. This process was maintained for 90, 180, 360 and 540 min, a thus tungsten coating with different thickness values was obtained. Other details of the coating preparation are described in Refs. [25].

Diamond/Cu composites with about 65 vol% of the coated diamond powers were fabricated via pressureless infiltration in a vacuum of 10^{-2} Pa. Before the infiltration, the uniform distribution of the reinforcement materials was ensured by measuring tap density. The tungsten-coated diamond particles were packed in a graphite mould to form a diamond particle bed. A wire mesh cover was placed into a graphite mould, and Cu was placed on the wire mesh cover. The effect of preparation parameters was eliminated by preparing the packed diamond with various tungsten coatings in the same graphite mould. A schematic of the pressureless infiltration unit is shown in Fig. 1. The graphite mould with diamond particles and Cu was then heated in the carbon tube sintering furnace (WZDS-20, Beijing Research Center) to 1350 °C with a heating rate of 26.6 °C/min for 45 min under vacuum status (<10^{-2} Pa). The graphite mould was naturally cooled to room temperature in the

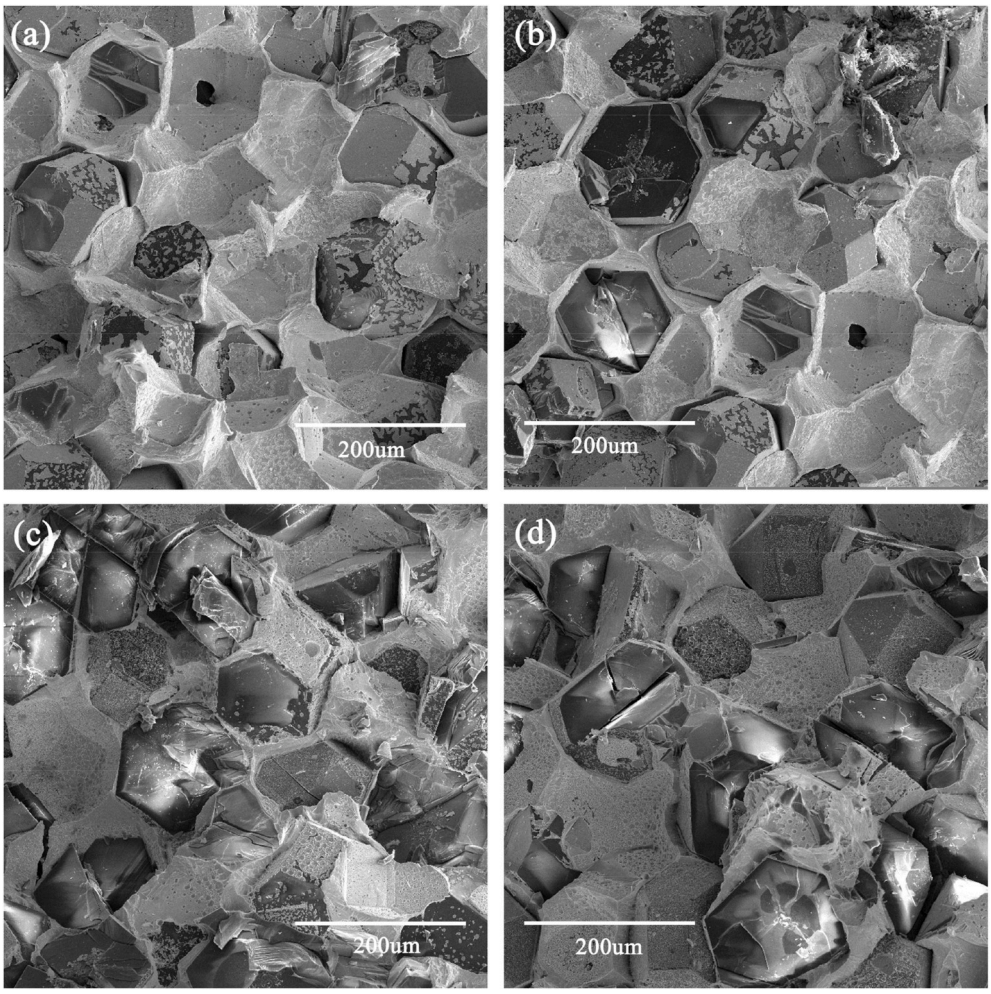

Fig. 6. SEM images of the fracture surfaces of the diamond/Cu composites with different coating thickness: (a) 45 nm, (b) 93 nm, (c) 218 nm, (d) 300 nm.

furnace. Disc-shaped composite samples with a diameter of 12.7 mm and height of 3 mm were obtained. Materials and processing conditions are summarised in Table 1 in which the composites with approximately 45, 93, 218 and 300 nm tungsten coatings were denoted as 'A', 'B', 'C' and 'D', respectively.

The microstructure of the coated diamond particles and the diamond/Cu composites were observed by an S4800 scanning electron microscope (SEM) equipped with energy dispersive spectroscopy. Atomic force microscopy (AFM) was performed on Dimension Icon to measure the roughness of the tungsten coatings. The interior structural information of diamond/Cu composites was analysed using an NDT/analyser high-energy X-ray nondestructive detection system. The thermal conductivity of composites was measured using a Netzsch LFA427 laser flash machine. A helium mass spectrometry leak detector ZQJ−542 was used to measure gas tightness. The XPS spectrum was obtained from Krators AXIS Ultra DLD via the X-ray radiation of 1253.6 eV Mg Ka to analyse the chemical state of the coatings. The phase constitutions of the coated diamond particles were examined via X-ray diffraction (D/maX 2550 VB + X-ray diffraction).

3. Test results and discussions

3.1. Formation of the tungsten coatings on diamond particles

The thickness AFM and SEM analyses were performed to investigate the surface morphology of the coatings. The thickness of coatings determined by gravimetric data was obtained by accurately comparing the mass of diamond particles before and after sputtering. The thickness of coatings was calculated under the assumption that each diamond particle is a sphere with the same size. The calculated results were higher than the actual results because the coatings were thin, and some particles were lost during sputtering.

The thickness of coatings was detected by breaking the coated diamond particles via thermal vibration combined with mechanical crushing. Subsequently, the exposed cross section was characterised via SEM to acquire coating thickness. The representative observation of the thickness of coatings is shown in Fig. 2 a–c. The profiles of the thickness indicate that the average thickness values of the coatings for 180, 360 and 540 min were approximately 93, 218 and 300 nm, respectively. The thickness of coatings approximately linearly increased with sputtering time. The coating thickness was approximately 45 nm when the sputtering time was 90 min by fitting to least squares. Typical SEM pictures of a diamond particle magnetron sputtered for 90 180, 360 and 540 min are presented in Fig. 2 a–d. A pronounced resemblance in the morphology of the coated diamond particles was exhibited with various magnetron sputtering times. The diamond particle was fully covered, and the coatings were smooth and dense. Moreover, high magnification image (Fig. 2 d) revealed that the diamond particles were evenly covered by submicron particles, and no observable voids were found.

Fig. 3 a shows the same image as Fig. 2 d in three dimensions and reveals a continuously lumpy character. The FAM observation (Fig. 3 b) topographical image clearly shows nanosized particles, confirming the surface morphology obtained from SEM and highlighting the presence of nanocrystalline particles.

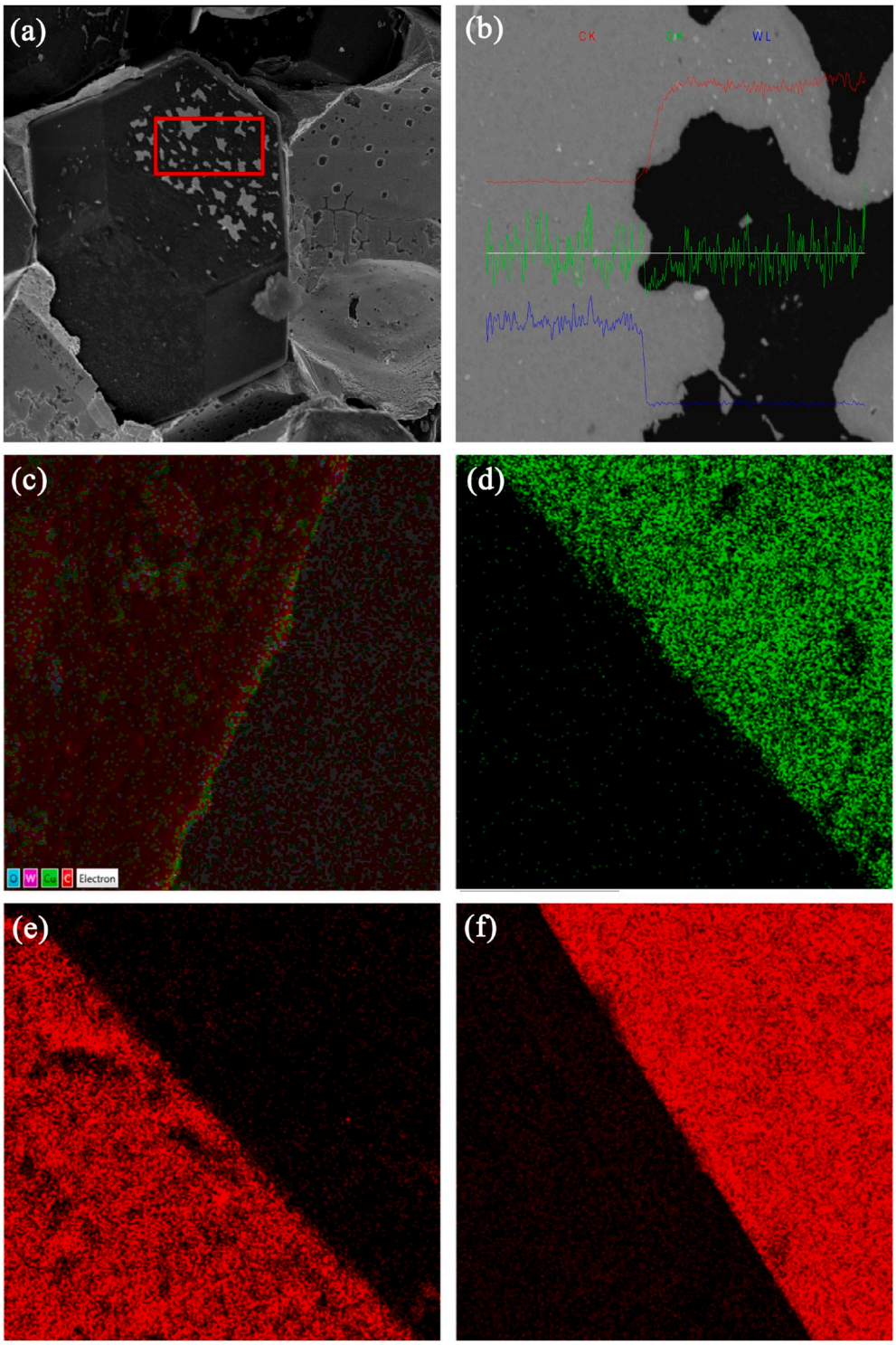

Fig. 7. EDS analysis: (a) the magnified image of fracture surfaces of composite A, (b) The EDS line-scanning analysis of the coated diamond surface from composite A, (c) EDS element distribution mappings of composite A, (d) (e) and (f) EDS mapping distributions of C of composite B, C and D.

The peak to peak (Ry), mean roughness (Ra) and ten-point height (Rz) of the coating measured by AFM were 6.8, 0.45 and 3.4 nm, respectively. These values indicate a small disordered region between peaks and valleys on the coating surface. Abyzov et al. [3,18] reported that a tungsten-based coating of 100 nm was prepared on the surface of diamond particles via diffusion treatment. However, the Ra of the surface was 37 nm, which is unfavourable for the TC properties because the electron transport at the metal interfaces is controlled by elastic scattering by disorder. Thus, magnetron sputtering can be a suitable method for preparing reliable tungsten coatings.

3.2. XRD and XPS analysis

In this work, XRD characterised the filler particles as a whole, and XPS spectra captured the local near-surface region. XRD analysis of diamond particles with different coating thicknesses are presented in Fig. 4. The three main peaks at $2\theta = 40^{\circ}$, 44° and 74° correspond to the (110), (200) and (211) crystal planes of a body-centred cubic tungsten,

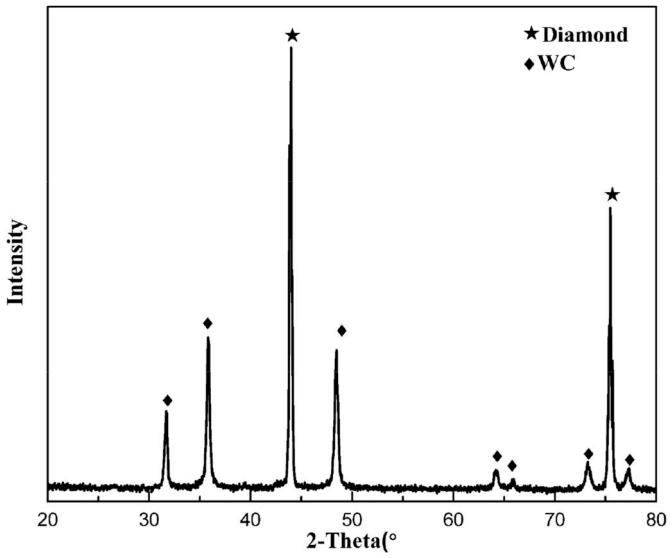

Fig. 8. XRD pattern of diamond particles with 300 nm coating underwent infiltration process.

respectively. It indicated that the reaction temperature between tungsten and diamond did not occur at the preparation temperature (300 °C), and no carbide was formed during magnetron sputtering.

The composition and bonding states of the coatings were further characterised by XPS. Fig. 5 shows the XPS fitted results of tungsten 4f from the coating. The symmetry peak at 35.7 and 37.8 eV in the W 4f spectrum were consistent with the characteristics of hexavalent tungsten with intermediate oxidation states based on the NIST XPS database [26–29]. The two lower binding energy peaks of tungsten 4f located at 31.1 and 33.2 eV exhibited that zero-valent tungsten could be verified, which is in conformity with the XRD results. The bond of W–O and W–W was the main bonding mode, and no substantial carbonisation formed during magnetron sputtering. The combined XPS and XRD analyses proved that a coating with a dominant tungsten phase and the bond of W–W and W–O was the main bonding mode on the coating surface. Details of the analysis are provided in Ref. [25].

3.3. Microstructure of diamond/Cu composites

Fig. 6 displays the microstructure of bending fracture surfaces of the composite samples. In the fracture mode, the coated diamond was often pulled out from the matrix and the ductile fracture of Cu [29]. However, the composites exhibited considerably different fracture morphologies with respect to various coating thicknesses. Fig. 6 c and d show that the diamond particles were distributed in the Cu matrix uniformly and integrated compactly with the Cu matrix through the carbides as a binder. This phenomenon explains why coatings guarantee the good adhesion between the diamond and the Cu matrix to form a strong mechanical interlocking. Strong interfacial bonding was obtained when WC Cr_7C3, Mo_2C and B_4C were utilised as coating [22,30–33]. The fracture surface of composites C and D (Fig. 6 c and d) was distinctive. Almost all diamond particles exhibited transcrystalline fractures, indicating a suitable coating thickness can ensure a strong interfacial bonding between the filler and the matrix. By contrast, Fig. 6 a–b show that the interface gap is evident between the reinforcements and the Cu matrix, suggesting a weak mechanical bonding between the diamond and the Cu matrix. Moreover, bare diamond surfaces were observed on the fracture surface of the coated diamond/Cu composites, as shown in Fig. 6 a and b, leading to the diamond particles being intact.

The typical diamond particle from composite A, as shown in Fig. 7 a, and the EDS line-scanning analysis in Fig. 7 b further confirm that the coating on the diamond particles was discrete irregular carbides. Fig. 7 c–f show the EDS mapping analysis of the cross-sectional microstructures of diamond/Cu composites as a representative. A good interfacial adhesion can be observed in Fig. 7 d–f. Moreover, the interface was straight and overlapped, indicating that the coating morphology was stable during infiltration, and the interface became flatter as the thickness of the coating increased.

XRD analysis shows that only WC and diamond existed in the diamond particles extricated from composite D (Fig. 8). Combined with the XRD results of ref [24], it can be confirmed that different thickness coatings were completely converted to WC. The typical diamond particle from composite A, as shown in Fig. 7a, and the EDS line-scanning analysis in Fig. 7 b further confirm that the coating on the diamond particles was discrete irregular carbides. The interface was prone to contraction and separation along the bare diamond surface due to the existence of the sparse coating surface, leaving behind the micropores. Therefore, producing a bond of low thermal resistance and a full metallurgical bonding between the reinforcement and the Cu matrix is difficult.

Fig. 9 shows the X-ray CT image of the diamond/Cu composite samples. The diamond particles were distributed in the Cu matrix uniformly in Fig. 9 c and d, which is consistent with those in the SEM image (Fig. 6 c and d). With the decrease in coating thickness, the coatings gradually broke up. Liquid Cu phase allows for the aggregation of floating particles and a descending Cu-rich zone, as shown in Fig. 9 b. The inner structure of composite A is similar to that of composite B, as shown in Fig. 9 a and b. The only difference is that a few pores exist inside composite A, indicating that the homogeneity of diamond/Cu composites is worsened with the decrease of coating thickness. It is understood that the fracture surfaces of composite A is strongly influenced by porosity. When the thickness increased to approximately 93 nm, microstructure gets worse due to the following reasons: firstly, diamond particles with thin coatings are prone to interfacial failure due to shrinkage and rupture of coatings. As a result, carbon affinity becomes poor, inducing the rearrangement of diamond particles. Secondly, the difference in the density of Cu and coated diamond is greater due to the relative long contact time at high temperature; thus, the diamond particles are easy to shift. Thirdly, the currently used infiltration temperature of 1300 °C could decreased to liquid Cu viscosity, which facilitate diamond particles to float during pressureless infiltration. Therefore, according to the infiltration kinetics, it is essential to increase the coating thickness and increase the contact time between diamond particles and copper melt to yield diamond/copper composites with homogenous microstructure.

3.4. Properties of diamond/Cu composites

Experimentally obtained properties of diamond/Cu composites with various coatings are shown in Table 1. The resulting composites had thermal conductivity values ranging from 487 W m^{-1} K^{-1} to 807 W m^{-1} K^{-1}. The thermal conductivity of composites firstly increased and then decreased with the increase in coating thickness. The highest thermal conductivity of 796 ± 11 W m^{-1} K^{-1} was achieved in the case of composites with 218 nm coatings. Further increment in the thickness of tungsten coating led to the TC value of the composite decreasing by 8.1% because the thick coating layer introduced a large interfacial thermal resistance. In the absence of shrinkage or rupture, the thinner the coating, the lower the interfacial thermal resistance. This behavior favoured improving thermal properties, but it was not a dominant factor in composite A. The lowest thermal conductivity value was measured in the case of composite A, which used the diamond with the 45 nm tungsten coating. The gas tightness data (Table 1) corresponding to the diamond/Cu system were consistent with the TC mentioned above. The gas tightness of composite A was approximately 5.1×10^{-8}, which is much higher than that of composites C and D. In the case of Al/diamond composites [14] fabricated by vacuum infiltration, tungsten coating with 45 nm was used to improve wettability and enhance the thermal

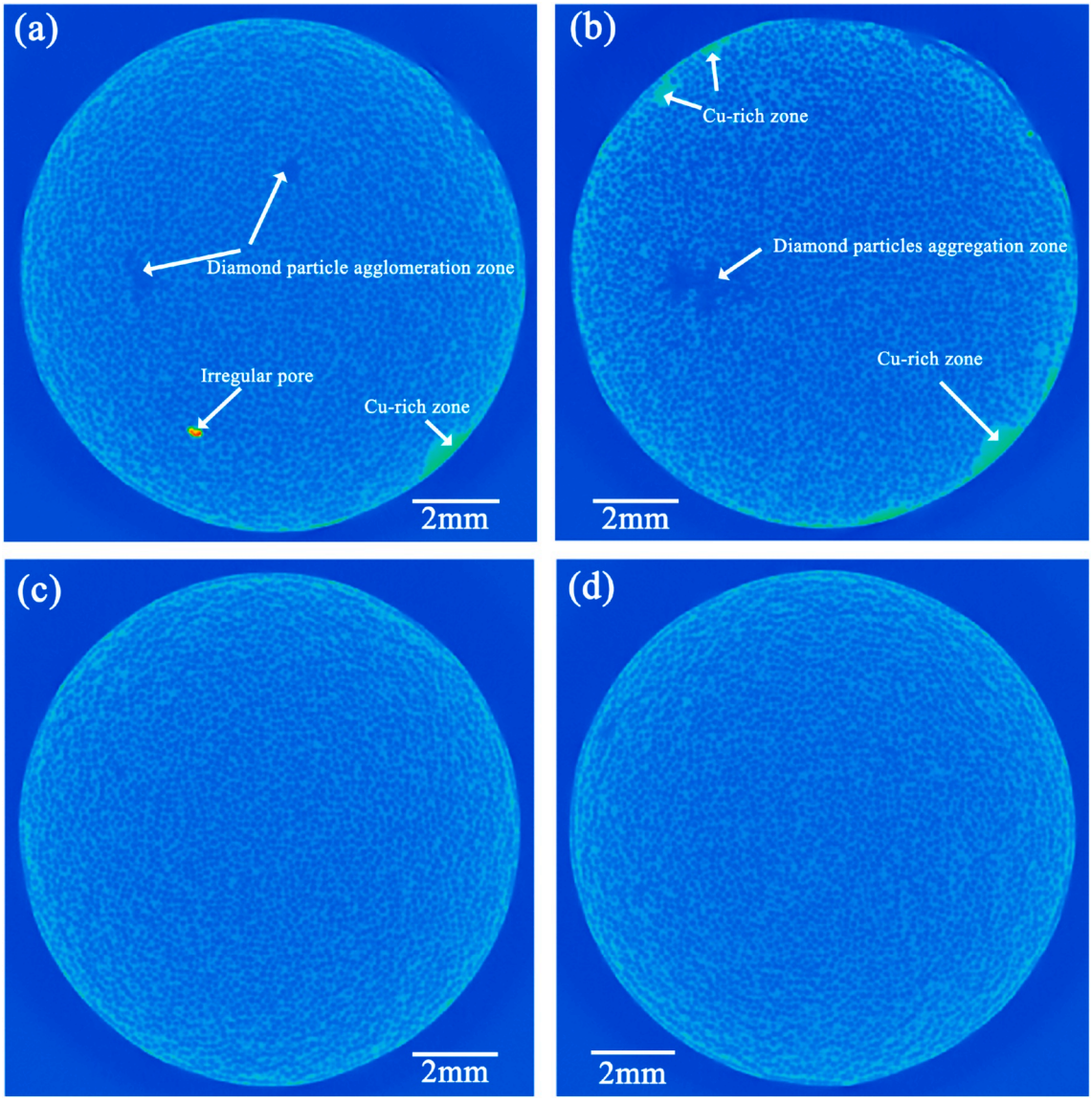

Fig. 9. X-ray imaging of diamond/Cu composites (a) with 45 nm coatings, (b) with 45 nm coatings, (c)with 218 nm coatings, (d) with 300 nm coatings.

Table 2
Parameters of materials for interfacial thermal resistance calculation.

Material	Density ($g \cdot cm^{-3}$)	Heat capacity ($J \cdot Kg^{-1} \cdot K^{-1}$)	Sound velocity ($m \cdot s^{-1}$)	Thermal conductivity ($W \cdot m^{-1} \cdot K^{-1}$)
Diamond	3520	510	12704	1500
Copper	8960	385	2970	400
WC	15700	355	4706	173

conductivity to a level of 622 W m^{-1} K^{-1}. Compared with microstructures, a bare diamond surface was not found in Al/diamond composites with 45 nm tungsten coatings because the liquid Al infiltration maintained a relatively low temperature (<900 °C), and the reaction between W and diamond occurred above 983.6 °C, which was lower than the reaction temperature between tungsten and diamond (≧983.6 °C) [22]. These results suggest that the decreased thermal conductivity of composite A can be attributed to the added internal microdefects, which effectively hinder the heat-conducting flow. Thus, the optimal values of tungsten coating thickness prepared by magnetron sputtering for forming diamond/Cu composites should exceed 93 nm. Composite D has further potential because it achieved a relatively high thermal conductivity, especially considering its relatively low leak rate.

We considered the incompleteness of the tungsten carbide interface. Based on the Hasselman and Johnson (H-J) model [34]. The interfacial thermal resistance (R_C) can be deduced using measured values, which can be written as:

$$R_c = \frac{a}{\lambda_{Dia}} \times \left[\frac{V_{Dia} \times \left(\frac{\lambda_{Dia}}{\lambda_{Cu}} - 1\right)\left(2 + \frac{\lambda_C}{\lambda_{Cu}}\right) + \left(2 + \frac{\lambda_{Dia}}{\lambda_{Cu}}\right)\left(1 - \frac{\lambda_C}{\lambda_{Cu}}\right)}{V_{Dia} \times \left(2 + \frac{\lambda_C}{\lambda_{Cu}}\right) + \frac{2\lambda_C}{\lambda_{Cu}} - 2} \right] \quad (1)$$

where λ_C, λ_{Cu} and λ_{Dia} are the effective thermal conductivities of the composite, Cu matrix ($\lambda_{Cu} = 400$) and diamond particles ($\lambda_{Dia} = 1500$) respectively; V_{Dia} is the volume fraction of diamond particles (65%); a is the average radius (180 μm) of the reinforcement.

The calculated results are shown in Table 1. Both an unusual decrease in the interface thermal resistance of the composite with an increase of the coating thickness, and a predictable increase in interface thermal resistance with increasing thickness were observed. The interface thermal resistance values deduced from H-J moldel of the three diamond/Cu composites (A, B and C) slightly decreased with the

increase in coating thickness. To the best of the authors' knowledge, the weaker the adhesion at the interface between the coated diamond and Cu, the lower the strength of the composite and the higher the thermal resistance of the interface. Combined with previous research findings [25], the high thermal conductivity obtained was associated with appropriate interface thickness and good composite density.

Meanwhile, the analysis thermal resistance of the perfect boundary can be analogous to a series circuit in which the total thermal resistance is composed by the sum of three terms ($R_c = R_{WC/Cu} + R_{Diamond/WC} + R_{WC}$): diamond/WC interface $R_{Diamond/WC}$, WC/Cu interface $R_{WC/Cu}$ and the resistance of the WC layer itself R_{WC}. Interface thermal resistance $R_{WC/Cu}$, $R_{Diamond/Cu}$ and $R_{Diamond/WC}$ can be calculated using the acoustic mismatch mode (Eq. (2)) [35,36].

$$R = \frac{2\left(\rho_m \nu_m + \rho_p \nu_p\right)^2}{C_m \cdot \rho_m^2 \cdot \nu_m^2 \cdot \rho_p \cdot \nu_p} \left(\frac{\nu_p}{\nu_m}\right)^2 \quad (2)$$

where ρ, C and ν are the density, specific heat capacity and Debye velocity of the matrix (longitudinal or transverse). Subscripts m and p refer to materials on the matrix and diamond side. R_{WC} was calculated by Eq $R_{WC} = L/\lambda$, where L is the average thickness of tungsten, which was recalculated into the average thickness of corresponding carbide. Table 2 lists the related data used in calculations based on Refs [25]. Amongst the composites, composite D had the highest Rc (2.24×10^{-9} $m^2 \cdot KW^{-1}$), and composite A had the lowest Rc (0.77×10^{-9} $m^2 \cdot KW^{-1}$). The obtained result implies that the thermal transport across interface is the most efficient in composite A, but composite A has the lowest thermal conductivity. The results only reflect a perfect bonding condition because they ignored the gap between discrete carbides. Thus, a thin coating could deteriorate the thermal conductivity of composites because a volume contraction and discontinuous carbide layer could not effectively improve the interfacial bonding of the composites.

4. Conclusion

Tungsten coatings with different thicknesses were deposited onto diamond particles via magnetron sputtering, and diamond/Cu composites were successfully fabricated via pressureless infiltration. A thickness of 218 nm is the optimum combination to improve the densification of overall composites and minimize the thermal boundary resistance between diamond particles and copper. Meanwhile, the densification of overall composites was improved with thick coatings, and the gas tightness reached 2.1 Pa m^3 s^{-1} with a 300 nm tungsten coating. Decreasing the coating thickness to 93 nm will worsen the interfacial bonding, resulting in the heterogeneous microstructure and performance degradation. The lowest thermal resistance of the diamond-WC-copper interface is 3.75×10^{-8} m^2 KW^{-1} in accordance with the calculations using the H-J model.

Declaration of competing interest

The authors declare that they have no known competing financial interests or personal relationships that could have appeared to influence the work reported in this paper.

CRediT authorship contribution statement

Jinhao Jia: Conceptualization, Methodology, Investigation, Writing - original draft. **Shuxin Bai:** Conceptualization, Methodology, Resources, Writing - original draft. **Degan Xiong:** Formal analysis, Data curation, Writing - review & editing. **Jing Xiao:** Writing - review & editing. **Tingnan Yan:** Writing - review & editing.

References

[1] M. Zhou, T. Lin, F. Huang, et al., Highly conductive porous graphene/ceramic composites for heat transfer and thermal energy storage, Adv. Funct. Mater. 23 (2013) 2263–2269.
[2] C. Zweben, Advances in composite materials for thermal management in electronic packaging, JOM 50 (1998) 47–51.
[3] A.M. Abyzov, S.V. Kidalov, F.M. Shakhov, High thermal conductivity composite of diamond particles with tungsten coating in a copper matrix for heat sink application, Appl. Therm. Eng. 48 (2012) 72–80.
[4] Lee, C.H.U.N.G. MuTse, et al., High thermal conductive diamond/Ag-Ti composites fabricated by low-cost cold pressing and vacuum liquid sintering techniques, Diam. Relat. Mater. 44 (2014) 95–99.
[5] T. Schubert, L. Ciupiński, W. Zieliński, et al., Interfacial characterization of Cu/diamond composites prepared by powder metallurgy for heat sink applications, Scripta Mater. 58 (2008) 263–266.
[6] L. Weber, R. Tavangar, On the influence of active element content on the thermal conductivity and thermal expansion of Cu–X (X = Cr, B) diamond composites, Scripta Mater. 57 (2007) 988–991.
[7] K. Chu, C. Jia, H. Guo, et al., On the thermal conductivity of Cu-Zr/diamond composites, Mater. Des. 45 (2013) 36–42.
[8] W. Yongpeng, L. Jiangbo, W. Yan, et al., Critical effect and enhanced thermal conductivity of Cu-diamond composites reinforced with various diamond prepared by composite electroplating, Ceram. Int. 45 (2019) 13225–13234.
[9] H.J. Cho, Y.J. Kim, U. Erb, Thermal conductivity of copper-diamond composite materials produced by electrodeposition and the effect of TiC coatings on diamond particles, Composites, Part B. 155 (2018) 197–203.
[10] H. Chen, C. Jia, S. Li, Interfacial characterization and thermal conductivity of diamond/Cu composites prepared by two HPHT techniques, J. Mater. Sci. 47 (2012) 3367–3375.
[11] Q. Kang, X. He, S. Ren, et al., Microstructure and thermal properties of copper–diamond composites with tungsten carbide coating on diamond particles, Mater. Char. 105 (2015) 18–23.
[12] S. Ma, N. Zhao, C. Shi, et al., Mo2C coating on diamond: different effects on thermal conductivity of diamond/Al and diamond/Cu composites, Appl. Surf. Sci. 402 (2017) 372–383.
[13] C. Chen, H. Guo, K. Chu, et al., Thermal conductivity of diamond/copper composites with a bimodal distribution of diamond particle sizes prepared by pressure infiltration method, Rare Met. 30 (2011) 408–413.
[14] W. Yang, G. Chen, P. Wang, et al., Enhanced thermal conductivity in Diamond/Aluminum composites with tungsten coatings on diamond particles prepared by magnetron sputtering method, J. Alloys Compd. 726 (2017) 623–631.
[15] H. Hu, J. Kong, Improved thermal performance of diamond-copper composites with boron carbide coating, J. Mater. Eng. Perform. 23 (2014) 651–657.
[16] A.M. Abyzov, et al., Diamond-tungsten based coating-copper composites with high thermal conductivity produced by Pulse Plasma Sintering, Mater. Des. 76 (2015) 97–109.
[17] Y. Dong, R. Zhang, X. He, Z. Ye, X. Qu, Fabrication and infiltration kinetics analysis of Ti-coated diamond/copper composites with near-net-shape by pressureless infiltration, Mater. Sci. Eng., B 177 (2019) 1524–1530.
[18] A.M. Abyzov, S.V. Kidalov, F.M. Shakhov, High thermal conductivity composites consisting of diamond filler with tungsten coating and copper (silver) matrix, J. Mater. Sci. 46 (2011) 1424–1438.
[19] C. Zhang, R. Wang, Z. Cai, C. Peng, Y. Feng, L. Zhang, Effects of dual-layer coatings on microstructure and thermal conductivity of diamond/Cu composites prepared by vacuum hot pressing, Surf. Coating. Technol. 277 (2015) 299–307.
[20] T. Okada, K. Fukuoka, Y. Arata, et al., Tungsten carbide coating on diamond particles in molten mixture of Na2CO3 and NaCl, Diam. Relat. Mater. 52 (2015) 11–17.
[21] Ł. Ciupiński, et al., Design of interfacial Cr_3C_2 carbide layer via optimization of sintering parameters used to fabricate copper/diamond composites for thermal management applications, Mater. Des. 120 (2017) 170–185.
[22] A.M. Abyzov, J.K. Mirosław, C. Łukasz, et al., Diamond-tungsten based coating-copper composites with high thermal conductivity produced by Pulse Plasma Sintering, Mater. Des. 76 (2015) 97–109.
[23] W. Yang, K. Peng, L. Zhou, et al., Finite element simulation and experimental investigation on thermal conductivity of diamond/aluminium composites with imperfect interface, Comput. Mater. Sci. 83 (2014) 375–380.
[24] G. Chen, W. Yang, L. Xin, et al., Mechanical properties of Al matrix composite reinforced with diamond particles with W coatings prepared by the magnetron sputtering method, J. Alloys Compd. 75 (2018) 777–786.
[25] J. Jia, S. Bai, D. Xiong, et al., Effect of tungsten based coating characteristics on microstructure and thermal conductivity of diamond/Cu composites prepared by pressueless infiltration, Ceram. Int. 45 (2019) 10810–10818.
[26] Z. Tan, Z. Li, D. Xiong, et al., A predictive model for interfacial thermal conductance in surface metallized diamond aluminum matrix composites, Mater. Des. 55 (2014) 257–262.
[27] L. Ottaviano, F. Bussolotti, L. Lozzi, et al., Core level and valence band investigation of WO_3 thin films with synchrotron radiation, Thin Solid Films 436 (2003) 9–16.
[28] J.R. Rumble, D.M. Bickham, C.J. Powell, The NIST x-ray photoelectron spectroscopy database, Surf. Interface Anal. 19 (2010) 241–246.
[29] C.D. Wagner, A.V. Naumkin, A. Kraut-Vass, J.W. Allison, C.J. Powell, J. R. Rumble Jr., NIST Standard Reference Database 20, in: NIST XPS Database Version, vol. 3, 2003.

[30] A.M. Abyzova, F.M. Shakhov, A.I. Averkin, et al., Mechanical properties of a diamond-copper composite with high thermal conductivity, Mater. Des. 87 (2015) 527–539.
[31] Y.M. Fan, H. Guo, J. Xu, et al., Effects of boron on the microstructure and thermal properties of Cu/diamond composites prepared by pressure infiltration, Int. J. Miner. Metall. Mater. 18 (2011) 472–478.
[32] Q. Kang, X. He, S. Ren, et al., Preparation of copper-diamond composites with chromium carbide coatings on diamond particles for heat sink applications, Appl. Therm. Eng. 60 (2013) 423–429.
[33] Q. Kang, X. He, S. Ren, et al., Effect of molybdenum carbide intermediate layers on thermal properties of copper-diamond composites, J. Alloys Compd. 576 (2013) 380–385.
[34] D.P.H. Hasselman, L.F. Johnson, Effective thermal conductivity of composites with interfacial thermal barrier resistance, J. Compos. Mater. 21 (1987) 508–515.
[35] E.T. Swartz, R.O. Pohl, Thermal boundary resistance, Rev. Mod. Phys. 61 (1989) 605–668.
[36] T. Schubert, Ł. Ciupiński, W. Zieliński, A. Michalski, T. Weißgärber, B. KiebackInterfacial characterization of Cu/diamond composites prepared by powder metallurgy for heat sink applications, Scripta Mater. 58 (2008) 263–266.